

# Shape and size characterization of potassium titanate fibers by image analysis

NINGZHONG BAO\*

*College of Chemical Engineering, Nanjing University of Technology, Nanjing 210009, People's Republic of China; Research Laboratory of Hydrothermal Chemistry, Kochi University, 2-5-1 Akebono-cho, Kochi 780-8520, Japan*  
E-mail: nzh\_bao@yahoo.com

LIMING SHEN

*College of Materials and Engineering, Nanjing University of Technology, Nanjing 210009, People's Republic of China*

XIN FENG, XIAOHUA LU\*

*College of Chemical Engineering, Nanjing University of Technology, Nanjing 210009, People's Republic of China*  
E-mail: xhlu@njuct.edu.cn

K. YANAGISAWA

*Research Laboratory of Hydrothermal Chemistry, Kochi University, 2-5-1 Akebono-cho, Kochi 780-8520, Japan*

The shape and size characterization of two types of potassium titanate fibers respectively prepared from anatase by the traditional calcination and from  $\text{TiO}_2 \cdot n\text{H}_2\text{O}$  by the promoted calcination were characterized by image analysis, showing distinguished advantages in description and comparison of shape of one dimensional materials. The accurate and quantitative relation of pixels of a digitized image to corresponding true size and the specifications, as well as the magnification of the image analysis system, and the horizontal resolving power and the scanning area of video-camera, of devices of the image analysis system, were found, which avoids the measuring deviation occurred in getting the relation between the pixels of a digitized image and corresponding true size from the digitized calibration graticule image in previous researches. Proposed image analysis parameters for characterizing shape and size of fibers were the length, the diameter, and the ratio of length to diameter, expressed by  $L_L$ ,  $L_D$ , and  $L_L/L_D$ , respectively. Fibers are defined those particles with  $L_L/L_D > 3$  for calculating the fiber content of a complex particle system. The non-fibrous particles were characterized using equivalent projected area diameter and the shape factor. The sampling method and the image analysis method proposed in the present study are generalized methods that can be applied for other fiber systems.

© 2004 Kluwer Academic Publishers

## 1. Introduction

Fibers have wide applications in composites, reinforcing materials and ceramics [1–5], where many colloid phenomena such as variations in agglomeration and flocculation have direct relation to shape and size of particles [6–11]. Many models [7] and simulations [8] about particles were established on the precise description of shape and size of particle phases. Potassium titanate fibers (PTFs), as well as  $\text{K}_2\text{Ti}_2\text{O}_5$ ,  $\text{K}_2\text{Ti}_4\text{O}_9$ , and  $\text{K}_2\text{Ti}_6\text{O}_{13}$ , are important functional materials that have been prepared industrially in large scale with low cost due to their economic importance and wide applications [12–17]. PTFs were mainly used as precursors

for preparing new titania-based fibers and as reinforcing agents for preparing high-performance composites and ceramics [1–5, 15–19], where the separation of PTFs from solution and performances of PTFs-based composites and ceramics all directly relate to the dispersity, which is influenced by the shape and size of PTFs, of PTFs in both solutions and composites. PTFs prepared from anatase by the traditional calcination are short with low fiber content and relatively high cost [14–17], while PTFs prepared from  $\text{TiO}_2 \cdot n\text{H}_2\text{O}$  by the promoted calcination are long with high fiber content and low cost [20, 21]. As a result, quantitative evaluation and description of shape and size of PTFs are required for

\*Authors to whom all correspondence should be addressed.

their optimal and effective applications and scientific researches.

Image analysis is the best method of observing a single particle for the shape description [22–26]. Recent advances of computer technology have made automatic image analysis fast, affordable, user-friendly, and increasingly common [27]. The statistical analysis for large amount of particles is the research trend and the focus of the image analysis, by which the true shape description was done [9]. Computer-aided image analysis has been widely used for the shape quantification because of both the increasing popularity of digital imaging and the development of efficient image processing algorithms that can be used to quantify complex shape [28]. However, the quantitative shape description of nonsphere-like particles is still hard to be done by the image analysis when compared with sphere-like particles [26]. Following four key problems need to be solved for the accurate image analysis of shape and size of fibers. (1) How to prepare representative sample slides; (2) How to obtain representative measuring results from sample slides; (3) How to get the accurate basic relation between the pixels of digitized image and corresponding true size; (4) Image reading and statistical analysis are very tired works but most important [9], and automatic analysis parameters are required for achieving proper and easy measurement and statistical analysis of fibers.

Problems 1 and 2 can be solved based on existing results [23, 24, 29, 31–34]. Various sampling methods have been proposed to obtain representative results based on the analysis to a certain amount of particles. If one hundred of measured visual areas, each containing six particles, on slides were imaged, 600 particles were measured to get the true size of sphere-like particles [31]. Wedd believed that the minimum number of particles measured for getting the representative results is  $>1500$  [32]. Barreiros found that the results measured from about 1500 particles or from a few hundreds of particles are same [29]. Vigneau got the reasonable result by measuring about 500 particles [33]. Actually, with the increase of the number of particle measured the average diameter approaches a constant representing the true size [34].

Whether the results of image analysis for non-sphere particles with special morphologies are accurate and reasonable is determined to the accuracy of image analysis, as well as proposed Problem 3, and selected image analysis parameters, as well as proposed Problem 4. For Problem 3, the accuracy of image analysis is determined to whether we can get the accurate relation of the pixels of digitized images to corresponding true size. In previous research, this quantitative relation was gotten from digitized images of a calibration graticule [27, 35] by correlating the pixels between two tick marks of standard unit in the calibration graticule image to the true size of this standard unit [29]. This relation was then used as the standard to make the size measurement for images imaged under condition the same as that of the calibration graticule image. However, the two tick marks of the standard unit in calibration graticule image are composed of various number of pixels due to

various imaging conditions, which makes it is hard for the operator to determine two terminal points, as well as two tick marks, of the standard unit manually. As a result, the pixel deviation occurs and is the main factor greatly influencing on the accuracy of image analysis in previous studies [25, 35]. Actually, in the present study, we find that the accurate and quantitative relation between the pixels and corresponding true size is only determined to specifications of devices of the image analysis system, and the measuring deviation due to the selection of two terminal points of the standard unit in previous studies can be avoided. For problem 4, no suitable image analysis parameters were proposed to characterize fibers in previous studies. In fact, fibrous particles have special shape, as well as large size in length, small size in diameter, and large ratio of length to diameter, which are characteristic shape properties for fibers and should be presented by suitable image analysis parameters.

In this work, the suitable sampling process for getting representative sample images was established based on standard methods [23, 24, 34]. The accurate and quantitative relation between the pixels and corresponding true size was correlated to specifications of devices of the image analysis system for avoiding the measuring deviation in previous image analysis. Automatic image analysis parameters were proposed for getting the true shape and size characterization of fibers. The characterization and comparison of shape and size of two types of PTFs were done by the established generalized image analysis.

## 2. Experiment

### 2.1. Materials

Standard  $\text{SiO}_2$  powders with equivalent diameter distribution of  $0.5\text{--}20\ \mu\text{m}$  and mid-value of gravimetric diameter of  $6.8 \pm 0.2\ \mu\text{m}$  were measured by sedimentation process. Two types of potassium titanate fibers designed “PTFs1” and “PTFs2” were respectively prepared from anatase by the traditional calcination [17] and from  $\text{TiO}_2 \cdot n\text{H}_2\text{O}$  by the promoted calcination [20, 21].

### 2.2. Instruments

Image analysis system consists of video camera (Panasonic-410, Matsushita Electric Industrial Co., Ltd., Japan), optical microscope (Galen III, Jiangnan Optical Instrument Co., Ltd., P. R. China), computer, and some connectors. The horizontal resolution and the scanning area of video-camera are 480 dpi (dot per inch) and  $4.9(\text{horizontal}) \times 3.7(\text{verticality})\ \text{mm}^2$ , respectively. Particle images with magnifications of 168, 420, 1680, and 4200 times can be obtained by this image analysis system. Ultrasonic disperse instrument was produced by Kunshan Ultrasonic Instruments Co., Ltd., P. R. China.

### 2.3. Experimental method

Standard  $\text{SiO}_2$  powders, PTFs1, and PTFs2, taken out from defined positions in sample bottles with standard methods [23, 24], were respectively dispersed in distilled water with 20-min ultrasonic wave in three

beakers. The gravimetric concentrations of SiO<sub>2</sub> powder, PTFs1, and PTFs2 all were 0.1% (wt%). The concentrations of sodium pyrophosphate for dispersing SiO<sub>2</sub> powders and of triethanolamine for dispersing PTFs were 0.2% (wt%). Five liquid drops were gathered at five symmetric places as well as the center, the surface, the bottom and two places approaching to the beaker wall, in a beaker. Each liquid drop was dropped at the center of a slide and covered with a cover glass. The slides containing single-layer well-dispersed particles were prepared after drying in vacuum.

Particles on slides were magnified by the image analysis system. Imaging places on a slide were the center place as the coordinate origin and four places extended along vertical and horizontal coordinate axis spaced fixed distance. As a result, five images were gotten from a slide.

### 3. Results and discussion

#### 3.1. Deviation study

Usually, for image analysis the quantitative pixel relation to true size was gotten from digitized images of a calibration graticule [35] by selecting the standard unit between two tick marks in a calibration graticule image manually [29]. This relation was used to make the size measurement for images imaged under the same condition. However, two tick marks of the standard unit in the calibration graticule image are composed of various number of pixels that are determined to the imaging condition, which makes it is hard for the operator to determine two terminal points of a calibration graticule in images manually. As a result, the pixel deviation occurred. In the present study, it is found that the relation between the pixels ( $n_s$ ) of a digitized image and corresponding true distance ( $U$ ,  $\mu\text{m}$ ) is determined to

specifications, as well as the magnification of the image analysis system ( $N$ ), and the horizontal resolving power (dpi) and the horizontal length of scanning area ( $\beta$ , mm) of video camera, of devices of the image analysis system. The quantitative functional relation is given by:

$$\begin{aligned} \frac{n_s}{\text{dpi}} &= \frac{(U (\mu\text{m}) \times N)/10000 \times 2.54}{(1 (\text{inch})/\beta (\text{mm}))/10 \times 2.54} \\ \Leftrightarrow n_s &= \frac{U (\mu\text{m}) \times N \times \beta (\text{mm}) \times \text{dpi}}{645160} \\ \Leftrightarrow \frac{U (\mu\text{m})}{n_s} &= \frac{645160}{N \times \beta (\text{mm}) \times \text{dpi}} \end{aligned} \quad (1)$$

Fig. 1 shows images of a calibration graticule at magnifications of 168, 420, 1680 and 4200 times. The true size between two adjacent tick marks is 10  $\mu\text{m}$ . The pixels of two tick marks ( $\overline{ab}$  and  $\overline{cd}$  see Fig. 1A–D) and the pixels between two adjacent tick marks ( $\overline{bc}$  in Fig. 1A–D) at different magnifications are counted manually and the results are listed in Table I. Table I also gives the quantitative relation of the pixels ( $n_s$ ) calculated by Equation 1 to 10  $\mu\text{m}$  distance at various magnifications.

From Table I, it is found that there are measuring deviations for the pixels ( $R$ ) counted manually when comparing with the pixels ( $n_s$ ) calculated by Equation 1. Also, the value of  $\frac{|R-n_s|}{n_s}$  decreases with the increase of the magnification ( $N$ ). These indicate that a large measuring deviation occurs at small magnifications if adopting the relation, obtained by manual counting of researchers, of the pixels to the true size in image analysis. It is also found that two tick marks of calibration graticule consist of various numbers of pixels at different magnifications, as shown in Table II. As a result,

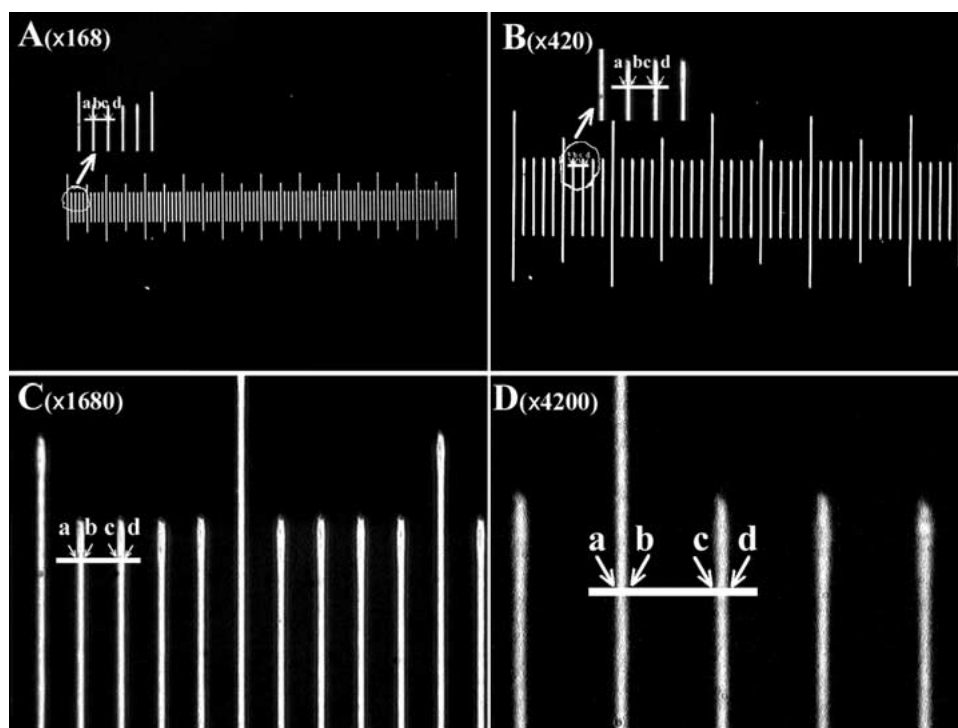


Figure 1 Images of calibration graticule at magnifications of (A) 168, (B) 420, (C) 1680, and (D) 4200 times. The distance between two adjacent vertical white tick marks in images A–D represents 10  $\mu\text{m}$ .

TABLE I The pixels of 10  $\mu\text{m}$  standard unit in digitized calibration graticule images, calculated by Equation 1 and counted manually at magnifications of 4200, 1680, 420, and 168 times<sup>a</sup>

$N$	$U$ ( $\mu\text{m}$ )	$P^b$ (pixel)	$Q^c$ (pixel)	$R^d$ (pixel)	$n_s$ (pixel)	$ \frac{R-n_s}{n_s} $ (%)
4200	10.0	20	113	153	153.12	0
1680	10.0	6	49	61	61.25	0.4
420	10.0	2	11	15	14.58	2.8
168	10.0	2	3	7	6.13	14.2

<sup>a</sup>  $P$ ,  $Q$ , and  $R$  were gotten manually, and  $n_s$  was calculated by Equation 1.

<sup>b</sup>  $P$ , the pixels of tick marks of calibration graticule (see  $ab$  and  $cd$  in Fig. 1A–D).

<sup>c</sup>  $Q$ , the internal width between two adjacent tick marks (see  $bc$  in Fig. 1A–D).

<sup>d</sup>  $R$ , the width of two tick marks of 10  $\mu\text{m}$  standard unit in digitized calibration graticule images and corresponding internal distance (see  $ad$  in Fig. 1A–D).

the deviations due to the selection of two tick marks of calibration graticule always exist and are determined to the operator's experience [25, 27, 35, 36]. On the contrary, the relation, obtained from Equation 1, between the pixels and corresponding true size gives the accurate size measurement, avoiding the previous measuring deviation due to the manual selection of two tick marks of calibration graticule.

## 3.2. Fiber characterization and measuring deviation study

### 3.2.1. Basic measuring parameters

Barreiros believed that the image analysis could not only measure the sphere-like particle size, but also evaluate the two-dimension shape factor, which were used for shape comparisons among different anisometric particles [29]. Similarly, the shape description of nonsphere-like particles was previously done by using of the equivalent diameter and corresponding shape factor for revising the shape. However, there were no existing image analysis parameters for the perfect and quantitative shape evaluation of one-dimensional fibers. In addition, different placed ways of fibers in images make it is difficult to perform the accurate shape and size characterization of fibers [36]. In the present study, suitable image analysis parameters, as well as the length ( $L$ ) and the diameter ( $D$ ), of fiber are proposed and shown in Fig. 2A. After digital image processing, the border of a

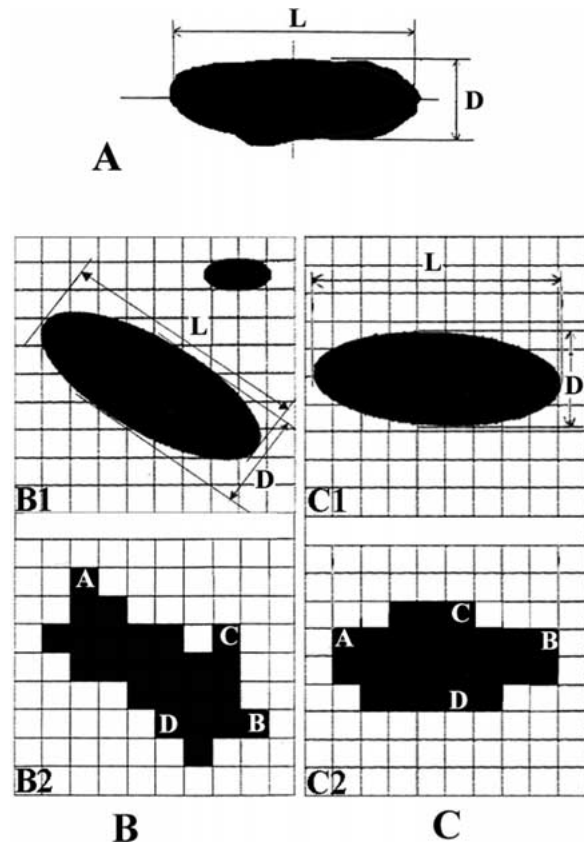


Figure 2 Quantitative image analysis parameters of a fiber. (A) Characteristic parameters of length ( $L$ ) and diameter ( $D$ ) of a schematic fiber. (B) Actual image (the inset B1) and digitized image (the inset B2) of the schematic fiber placed with a certain slope. (C) Actual image (the inset C1) and digitized image (the inset C2) of the schematic fiber placed horizontally.

digitalized fiber image is concavo-convex (see Fig. 2B2, C2). While, the border of original fiber is smooth (see Fig. 2B1, C1). As a result, traditional measuring parameters, such as the equivalent projective area diameter, the sphericity factor, and so on, will bring large measuring deviation. Further, for fibers the horizontal placed way (see Fig. 2C1, C2) generates smaller deviation than that of placed way of incline (see Fig. 2B1, B2). Nevertheless, these deviations can be decreased by using of the length ( $L$ ) and the diameter ( $D$ ) as image analysis parameters for fibers.

In this work,  $(X, Y)$  is used to describe a pixel position in an image.  $X, Y$  are defined as the horizontal

TABLE II Measuring deviations of length, diameter and ratio of length to diameter of fibers by proposed image analysis parameters on different size scales

$L$ ( $\mu\text{m}$ )	$D$ ( $\mu\text{m}$ )	$L_L$ ( $\mu\text{m}$ )	$L_{\text{dev}}$ (%)	$L_D$ ( $\mu\text{m}$ )	$ D_{\text{dev}} $ (%)	$L/D$	$K$	$K_{\text{dev}}$ (%)
1.00	0.50	1.12	11.80	0.45	10.60	2.00	2.50	25.00
	1.00	1.41	41.40	0.71	29.30	1.00	1.41	41.00
3.00	0.50	3.04	1.30	0.51	2.00	6.00	6.00	1.63
	1.00	3.16	5.30	1.05	5.00	3.00	3.00	6.25
5.00	0.50	5.03	0.50	0.50	0.40	10.00	10.09	0.90
	1.00	5.10	2.00	0.98	1.90	5.00	5.20	4.00
10.00	0.50	10.01	0.13	0.50	0.20	20.00	20.07	0.35
	1.00	10.03	0.50	1.00	0.30	10.00	10.06	0.60
20.00	0.50	20.01	0.03	0.50	0.04	40.00	40.03	0.08
	1.00	20.13	0.13	0.99	0.60	20.00	20.27	1.35

$|D_{\text{dev}}|$ , absolute values.

and the vertical coordinates of each selected pixel, respectively. If a spatial calibration has been performed, the calibrated  $X$ ,  $Y$  coordinates are reported. If no spatial calibration has been made, the default raw image pixel coordinates are reported and  $X$ ,  $Y$  coordinates are reported in pixel relative to an origin in the lower left corner of the image.

The pixel ( $n_i$ ) between two pixels in an image is calculated by:

$$n_i = \sqrt{(X_2 - X_1)^2 + (Y_2 - Y_1)^2} \quad (2)$$

where  $X_1$  and  $Y_1$  are the horizontal and the vertical coordinates of one pixel, respectively, and  $X_2$  and  $Y_2$  are the horizontal and the vertical coordinates of another pixel, respectively.

The equivalent projected area diameter  $D_a$  and the sphericity factor  $SF$  are used to express the degree of irregularity of each particle, given by:

$$D_a = \sqrt{\frac{4 \times S_a}{\pi}} \quad (3)$$

$$SF = \frac{4\pi \times S_a}{p_e^2} \quad (4)$$

where,  $S_a$  and  $p_e$  are the projected area and the perimeter of a particle, respectively. The shape factor of a perfect circle is 1, and a line has a shape factor approaching 0.

The measured distance  $LE$  is given by:

$$LE = n_i \left( \frac{U}{n_s} \right) \quad (5)$$

where  $n_i$  is the pixel, measured by Equation 2, of a line;  $U/n_s$  is a constant that is determined to image analysis system, known from Equation 1.

In this work, sphere-like  $\text{SiO}_2$  particles are characterized statistically by image analysis. The characteristic parameters are the equivalent projective area diameter  $D_a$  and the sphericity factor  $SF$ , expressed by Equations 3 and 4, respectively.

### 3.2.2. Description of fibers

The true shape and size description of the fibers was done by the statistical image analysis of large amount of fibers. The length distribution, the diameter distribution, and the ratio of the length to the diameter are perfect parameters for the shape characterization of an individual fiber.  $L_L$  and  $L_D$  are proposed to represent the length and the diameter of a fiber, respectively. In a fiber image,  $L_L$  is defined the maximum length of a straight line connecting two points on the border of fiber image. For example,  $L = L_L = \overline{AB}$  (see Fig. 2B2, C2).  $L_D$  is defined the maximum length of a straight line vertical to the straight line with the length of  $L_L$  and connecting two points on the border of fiber image. For example,  $D = L_D = \overline{CD}$  (see Fig. 2B2, C2). The quantitative relation between the true distance and corresponding pixels is calculated by Equation 5. The measuring parameters of  $L_L$  and  $L_D$  for fibers are thus

expressed by following Equations 6 and 7.

$$L_L = \frac{U}{n_s} \sqrt{(X_{2L} - X_{1L})^2 + (Y_{2L} - Y_{1L})^2} \quad (6)$$

$$L_D = \frac{U}{n_s} \sqrt{(X_{2D} - X_{1D})^2 + (Y_{2D} - Y_{1D})^2} \quad (7)$$

where  $(X_{1L}, Y_{1L})$  and  $(X_{2L}, Y_{2L})$  respectively are coordinates of two terminal pixels of the straight line of  $L_L$ .  $(X_{1D}, Y_{1D})$  and  $(X_{2D}, Y_{2D})$  respectively are two coordinates of two terminal pixels of the straight line of  $L_D$ .

There exist deviations between the measured values ( $L_L$ ,  $\overline{AB}$  in Fig. 2B2, C2, and  $L_D$ ,  $\overline{CD}$  in Fig. 2B2, C2) and corresponding true values ( $L$  and  $D$ , in Fig. 2B1, C1). If a fiber is treated as a rectangle ( $A \times B$ , where  $A$  and  $B$  represent the length and the width, respectively), measuring deviations of the length and the diameter of fibers by proposed image analysis parameters of  $L_L$  and  $L_D$  are given as following.

$$L_L = \sqrt{A^2 + B^2} \quad (8)$$

$$L_D = \frac{B}{A} \sqrt{A^2 + B^2} \quad (9)$$

$$K = \frac{L_L}{L_D} \quad (10)$$

$$L_{\text{dev}} = \frac{L_L - A}{A} \times 100(\%) \quad (11)$$

$$D_{\text{dev}} = \frac{L_D - B}{B} \times 100(\%) \quad (12)$$

$$K_{\text{dev}} = \frac{K - \frac{A}{B}}{\frac{A}{B}} \times 100(\%) \quad (13)$$

where,  $L_L$ ,  $L_D$  and  $K$  are measured values representing the length, the diameter and the ratio of the length to the diameter, respectively, and  $L_{\text{dev}}$ ,  $D_{\text{dev}}$ , and  $K_{\text{dev}}$  are corresponding measuring deviations that were listed in Table II on various size ranges. It is found that for a constant diameter ( $L_D$ ), the measuring deviation of the length decreases with increase of the measured length ( $L_L$ ), which is the same to the diameter ( $L_D$ ) at a constant length ( $L_L$ ). According to Table III, particles with diameters of 0.5–1.0  $\mu\text{m}$  and  $L_L > 3 \mu\text{m}$ , or  $K > 3.0$ , are defined as fibers. For this part of particles, the measuring deviation is lower than 5%, indicating an accurate image analysis of fibers. The left particles are defined as non-fibrous particles that are described by using the same method as that for sphere-like particles.

TABLE III Overall image analysis results for Slides 1–5#

Slide	Particle number	Average diameter $D_a$ ( $\mu\text{m}$ )	Total particle number	Average $D_a$ ( $\mu\text{m}$ )	Standard deviation
1	44	7.17			
2	40	7.16			
3	43	7.50	233	7.30	0.2413
4	66	7.11			
5	40	7.65			

The image analysis of the fiber system is divided into two steps. One step is the measurement for the content of non-fibrous particles that can be characterized as sphere-like particles [29, 37]. The next step is the shape and size characterization of defined fibers with proposed image analysis parameters.

### 3.3. Image analysis of SiO<sub>2</sub> and PTFs

#### 3.3.1. Images of powders

Standard SiO<sub>2</sub> particles and two types of PTFs were imaged by the image analysis system, and corresponding representative images are shown in Fig. 3. Most standard SiO<sub>2</sub> particles are sphere-like (see Fig. 3A). The observation comparison between Fig. 3B and C shows that the fiber content of PTFs2 are larger than that of PTFs1, and fibers in PTFs2 are longer than those of PTFs1. The length and the diameter of fibers in PTFs2 are uniform. The qualitative analysis for particle shape

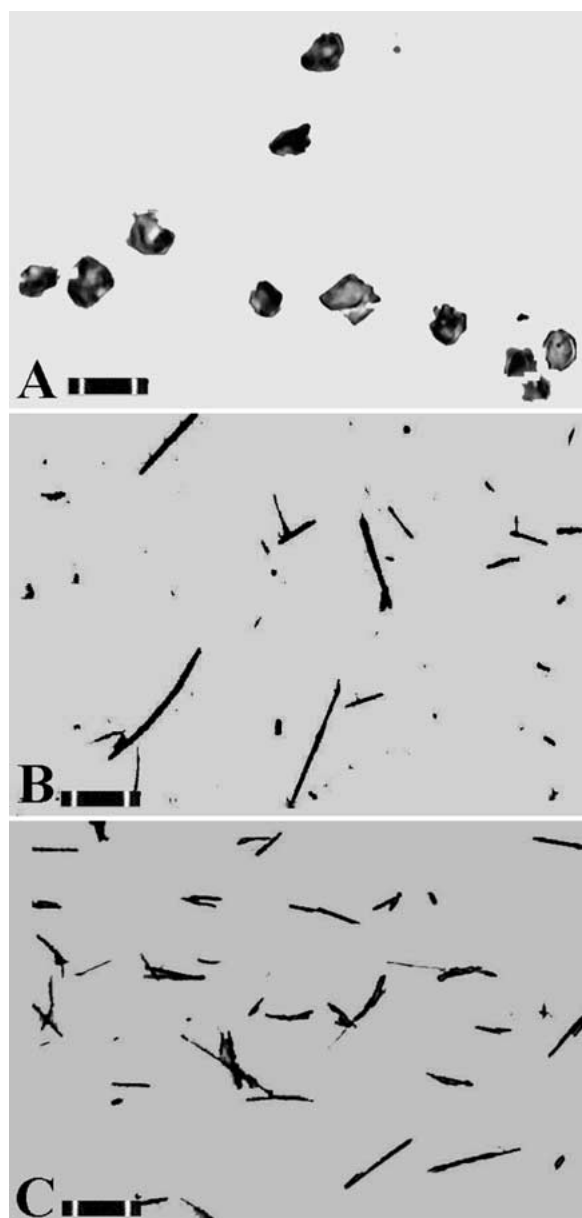


Figure 3 Images of SiO<sub>2</sub> (A), PTFs1 (B) and PTFs2 (C) at magnification of 1680 times obtained by image analysis system. The scale bars for all images are 10 μm.

can only be done by the visual comparison to particle images.

#### 3.3.2. Image analysis of standard sphere-like SiO<sub>2</sub> powders

The sampling and imaging method proposed to get representative slides was confirmed to be effective by the test to standard SiO<sub>2</sub> particles. According to the method proposed in Section 2.3, 25 viewing fields on 5 slides were imaged. Table III lists the analysis results. The shape factor distribution and the size distribution of standard SiO<sub>2</sub> powders are shown in Fig. 3.

In Table III, the values of average diameters ( $D_a$ ) of particles on slides 1–5 are close, which indicates that the well-dispersed representative particle slides were prepared by the proposed sampling method and the accurate size distribution was measured by the image analysis system. The statistical size was gotten as the measured particles number is >200, agreeing the particle number determination method for getting true size distribution reported by Vigneau [33]. Further, more particles over several thousands can also be analyzed by our image analysis system, automatically, easily, and quickly.

Fig. 4A shows the shape factor distribution of standard SiO<sub>2</sub> particles. The fitting result is expressed by.

$$Y = 0.1485 \ln X + 0.2942 \quad (14)$$

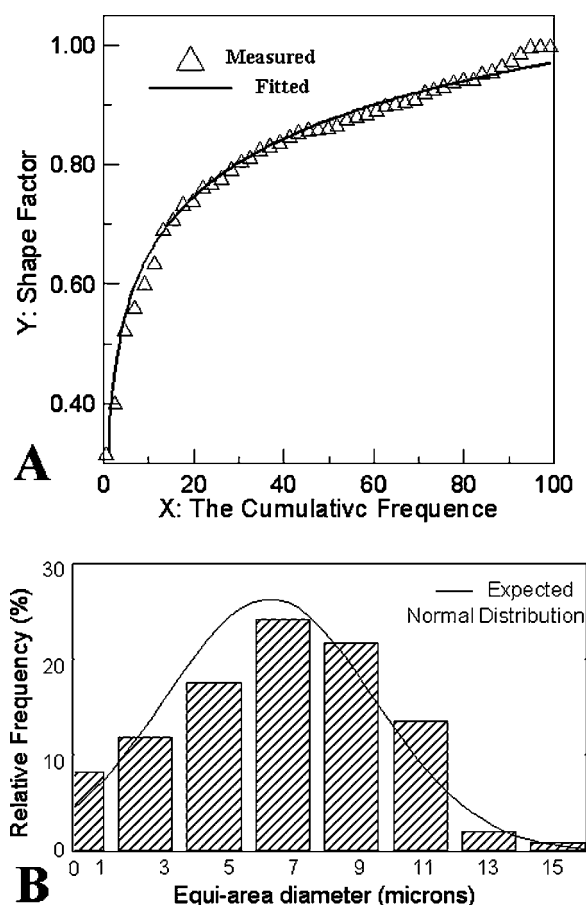


Figure 4 Shape factor distribution (A) and equivalent projected area diameter distribution (B) of standard SiO<sub>2</sub> particles, obtained by image analysis.

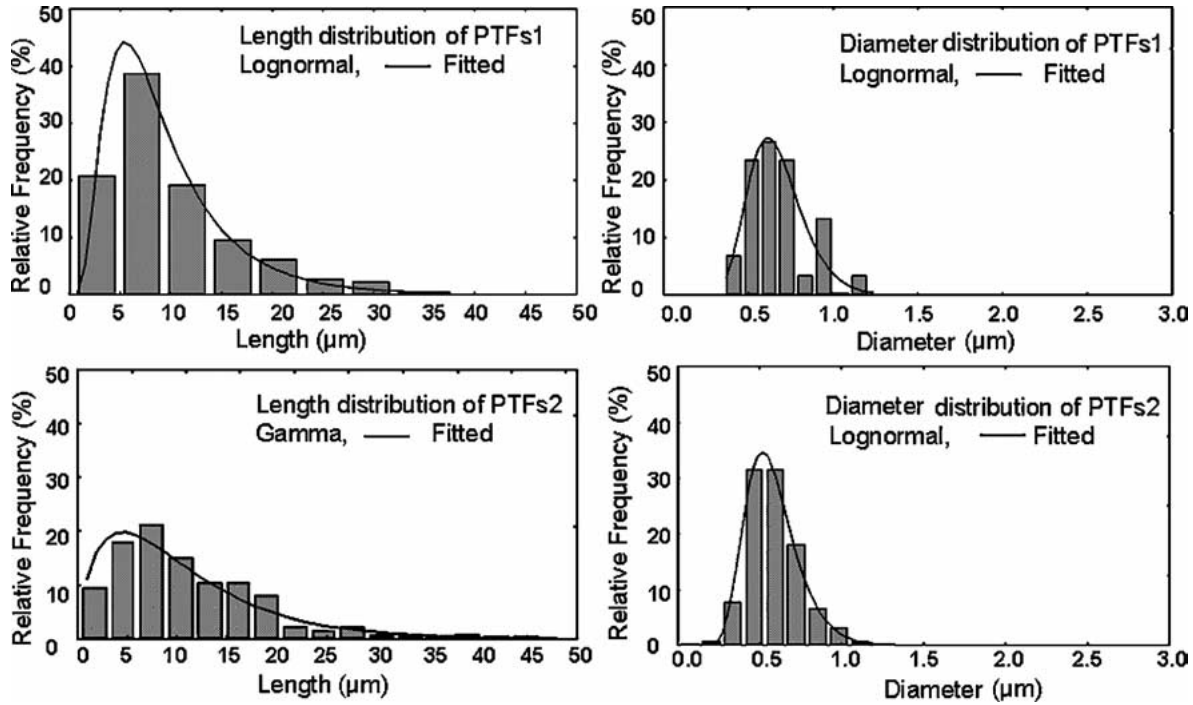


Figure 5 Length and diameter distributions of PTFs1 and PTFs2, obtained by image analysis.

The cumulative frequency of  $X$  is 15.37 when the shape factor of  $Y$  is 0.7, which indicates that 84.63% of standard  $\text{SiO}_2$  particles are sphere-like or global. The shape factor focuses on 0.7–1.0. Fig. 4B shows the normal distribution of the equivalent projected area diameter, focusing on 7  $\mu\text{m}$ . Corresponding normal distribution parameters are  $\mu$  of 6.83 and  $\sigma$  of 3.49, respectively.

### 3.3.3. Image analysis of PTFs

Quantitative analysis results showing detailed discriminations of shape and size of PTFs are obtained by image analysis, using proposed image analysis parameters, as well as the length ( $L_L$ ), the diameter ( $L_D$ ), and the ratio of the length to the diameter ( $K$ ). Because the average diameter of PTFs is  $< 1 \mu\text{m}$ , particles with  $L_L > 3.0 \mu\text{m}$  are defined the fibers.

For PTFs1,  $L_L$ ,  $L_D$ ,  $K$  and the fiber content are 9.58  $\mu\text{m}$ , 0.67  $\mu\text{m}$ , 14.30 and 47.4%, respectively; For PTFs2,  $L_L$ ,  $L_D$ ,  $K$  and the fiber content are 11.49  $\mu\text{m}$ , 0.58  $\mu\text{m}$ , 19.81 and 74.5%, respectively; The fiber content of PTFs2 is higher than that of PTFs1. The average diameter of PTFs2 is smaller than that of PTFs1. The average length and the average ratio ( $K$ ) of length to diameter of PTFs2 are larger than those of PTFs1. These results indicate that high quality PTFs were prepared by the promoted calcination [20, 21].

TABLE IV Parameters of functions of length and diameter distributions of PTFs1 and PTFs2

No.	Sample capacity	Distribution	Parameters
PTFs1	178	Length	Log-normal $\mu: -0.43$ $\sigma: 0.05$
		Diameter	Log-normal $\mu: 2.09$ $\sigma: 0.35$
PTFs2	296	Length	Gamma $\alpha: 11.49$ $\beta: 0.26$
		Diameter	Log-normal $\mu: -0.58$ $\sigma: 0.07$

Distributions of the length and the diameter of PTFs1 and PTFs2 are shown in Fig. 5. Distribution types in Fig. 5 are mainly log-normal

$$\text{Ln}(\mu, \sigma^2), \quad p_{\text{Ln}}(x) = \frac{1}{\sqrt{2\pi}\sigma x} e^{-\frac{(\ln x - \mu)^2}{2\sigma^2}}$$

and gamma distribution

$$\Gamma(\alpha, \beta), \quad p_{\Gamma}(x) = \frac{\beta^\alpha}{\Gamma(\alpha)} (x - c)^{\alpha-1} e^{-\beta(x-c)}.$$

The distribution parameters are calculated and shown in Table IV. The parameter  $\sigma$  reflects the discrete state of the distribution. A larger  $\sigma$  indicates more discrete of the distribution. For the length distribution of PTFs1, the value of  $\sigma$  is the smallest, so its length distribution is the narrowest. These are the same to the diameter distribution.

From Fig. 5 and Table IV, quantitative statistical analysis results obtained by proposed image analysis parameters for fibers show us many detailed quantitative comparisons, which cannot be described by direct image observation from Fig. 3B, C, for shape and size characterizations of two types of PTFs.

## 4. Conclusion

In the present study, the quantitative relation between the pixels and corresponding true size is determined to specifications of devices of image analysis system, which was used to do quantitative image analysis. The representative sample slides and image analysis results were gotten by our proposed sampling and image analysis method. The suitable image analysis parameters for the shape and size description of fibers are the length, the diameter, the ratio of length to diameter, and the content of the fiber. The fiber content was used to distinguish the fibers from a complex particle system.

Subsequently, the fibrous particles were described by using our proposed image analysis parameters. Application to two types of PTFs showed that the characterization and comparison of shape and size of fiber systems could be done by our proposed image analysis method accurately and quickly. The obtained quantitative image analysis results can be used in many models and simulations of complex particle systems and applications of composites and ceramics, too.

### Acknowledgements

Authors appreciate the Outstanding Youth Fund of National Natural Science Foundation (29925616), National High-tech Research Development Program (863 Program: 2003AA333010), Natural Science Foundation (20246002, 20236010), and The Tribology Science Fund of National Tribology Laboratory (SKLT02-2), of P. R. China, and the help and facilities of Research Laboratory of Hydrothermal Chemistry, Kochi University, Japan.

### References

1. J. LÜ and X. LU, *J. Appl. Polym. Sci.* **82** (2001) 368.
2. S. C. TJONG and Y. Z. MENG, *Polymer* **40** (1999) 1109.
3. J. HOMENY, Whisker reinforced Ceramics, in "Ceramic Matrix Composites," edited by W. Reachard (Blackie, Glasgow, UK, A Review, 1993) p. 240.
4. S. TARUTA, S. HIROKAWA, H. KAWAMURA and N. TAKUSAGAWA, *J. Ceram. Soc. Jpn.* **105** (1997) 1158.
5. M. SANDO, A. TOWATA and A. TSUGE, in "Ceramic Transactions," Vol. 22, edited by S. Hirano, G. L. Messing and H. Hausner (American Ceramic Society, Westerville, OH, 1991) p. 101.
6. A. S. BRAMLEY, M. J. HOUNSLOW and R. L. RYALL, *J. Coll. Interf. Sci.* **185** (1996) 155.
7. R. P. SEAR and G. JACKSON, *J. Chem. Phys.* **103** (1995) 8684.
8. S. STOLL and E. PEFFERKORN, *J. Coll. Interf. Sci.* **177** (1996) 192.
9. H. DEZ, J. BERT and J. DUPUY-PHILON, *ibid.* **185** (1997) 190.
10. E. L. KNUTH and U. HENNE, *J. Chem. Phys.* **110** (1999) 2264.
11. A. R. HENN, *Part. Part. Syst. Charact.* **13** (1996) 249.
12. R. MARCHAND, L. BROHAN, R. MBEDI and M. TOURNOUX, *Rev. Chim. Miner.* **21** (1984) 476.
13. A. CLEARFIELD, *Chem. Rev.* **88** (1988) 25.
14. T. SHIMIZU, *Industr. Chem. (Jpn.)* **5** (1980) 87; **7** (1980) 104.
15. H. KONUCHI and Y. NARITA, *Zeoraito (Japanese)* **9**(3) (1992) 103.
16. X. FENG, J. LU, X. LU, N. BAO and D. CHEN, *Acta Mater. Comp. Sinica* **16** (1999) 1.
17. N. BAO, X. FENG, X. LU and Z. YANG, *J. Mater. Sci.* **37**(14) (2002) 3035.
18. S. YIN and T. SATO, *Ind. Eng. Chem. Res.* **39** (2000) 4526.
19. N. BAO, X. LU, X. JI, X. FENG and J. XIE, *Fluid Phase Equilibria* **193** (2002) 229.
20. N. BAO, X. FENG, L. SHEN and X. LU, *Crystal Growth and Design* **2** (2002) 437.
21. N. BAO, X. FENG, L. SHEN, X. LU and Z. YANG, *J. Amer. Ceram. Soc.* in press.
22. A. SCHÜLE, W. RASEMANN and C. PREUBE, *Part. Part. Syst. Charact.* **14** (1997) 21.
23. C. HUANG (ed.), Handbook of Chemical Engineering—Particle and Particle System No. 19., Chemical Industry Press (in Chinese).
24. T. ALLEN (ed.), "Particle Size Measurement," 3rd ed. (Chapman & Hall, New York, 1987).
25. J. A. DAVIDSON, A. A. ETTER, M. THOMAS and R. S. BUTLER, *Part. Part. Syst. Charact.* **9** (1992) 94.
26. M. N. PONS, H. VIVIER, K. BELAROU, B. BERNARDMICHEL, F. CORDIER, D. OULHANA and J. A. DODDS, *Powder Technology* **103**(1) (1999) 44.
27. J. C. RUSS, "Image Processing Handbook," (CRC Press, Boca, FL, USA, 1992).
28. P. M. RAJ and W. R. CANNON, *Powder Technology* **104** (1999) 180.
29. F. M. BARREIROS, D. F. FERREIRA and M. M. FIGUEIREDO, *Part. Part. Syst. Charact.* **13** (1996) 368.
30. R. P. CHHABRA, L. AGARWAL and N. K. SINHA, *Powder Technology* **101** (1999) 288.
31. G. L. FAIRS, in "Particle Size Measurement," edited by T. Allen (Chapman & Hall, New York, 1987).
32. M. WEDD, Particle Sizing, in "Food Process Monitoring Systems" edited by A. C. Pinder and G. Godfre (Blackie Academic and Professional, 1993) p. 102.
33. E. VIGNEAU, C. LOISEL, M. F. DEVAUX and P. CANTONI, *Powder Technology* **107** (2000) 243.
34. R. R. IRANI, C. F. CALLIS and J. M. DALLEVALLE, "Particle Size" (Wiley, NY, 1963).
35. T. A. KRAMER and M. M. CLARK, *Part. Part. Syst. Charact.* **13** (1996) 3.
36. K. SUNADA, *Powder Sci. Engin. (Japanese)* **32**(2) (2000) 68.
37. S. ENDOH, Y. KUGA, H. OHYA, C. IKEDA and H. IWATA, *Part. Part. Syst. Charact.* **15** (1998) 145.

Received 15 April  
and accepted 9 September 2003